

In-situ Atomic-scale Matrix-Bracketing Blanks & Peak Overlap Correction for Ti-V-Cr in Diverse Tourmalines

Jared Wesley Singer¹ and Marian Lupulescu²

¹Troy, New York, United States, ²New York State Museum, Albany, New York, United States

This study gives a method for correction of the Ti-V-Cr peak overlaps and trace-level baselines for tourmalines by EPMA using a strategy of matrix-bracketing blanks. This case is a particular challenge for several reasons: 1) typical concentration levels are $Ti \gg V \gg Cr$, 2) chromium suffers loss of precision from the cascading double interference correction, 3) common reference materials for interference calibration are not matrix matched (e.g. V_2O_3 , Chromite), and 4) lack of high-purity tourmaline references which span wide range of compositions.

To circumvent the last of these issues, we solve the lack of ideal matrix-matched blanks using a population survey approach. LA-ICP-MS is used to rapidly identify candidate blanks from a compositionally diverse collection of natural tourmalines (mostly from New York State Museum and RPI collections). Of these a subset is identified based on particular characteristics such as homogeneity, having minimums and maximums of major elements (e.g. compositional bracketing), and critically, non-detectable levels ($<< 1$ ppm) of a particular trace element. The blank population defines a trend line in the bivariate plot (see figure 1), where the slope is due to peak overlap and the intercept due to baseline subtraction. This scheme is used in conjunction with software-based interference correction algorithms, or can be used alone for post-hoc adjustment in the trace element limit. Donovan et al. (1993) pointed out a common mistake of ZAF miscalculation related to peak overlap calibration--exacerbated when reference materials were not matrix-matched. We find persistent bias of peak overlap corrections in modern software and recommend this empirical approach to double-check theoretical data processing.

Significant disagreement persists for the absolute inter-calibration of EPMA and LA-ICP-MS (commonly 0 to 30% bias is observed). For primary calibration of EPMA we still rely on high purity oxides (e.g. TiO_2 , V_2O_3 , Chromite) calibrated at low beam current (~ 10 nA, but not 5 nA due to an observed instability at the 5 nA value). For LA-ICPMS we rely only on its fidelity to orders-of-magnitude (ppm $>$ ppb, etc.). The ICPMS baseline is defined by the time-resolved gas-blank of the plasma, and common artifacts such as isobaric and molecular interference result in false positives. Care must be given to ensure that there is a reasonable ablation yield (nice tracks) and not overloading the plasma (suppressed ionization). The combination of techniques results in especially useful synergy when utilizing EPMA for accurate quantification and LA-ICPMS for checking the zero point of EPMA. We find that optimal precision for Cr is maintained by ensuring equally precise measurement of all Ti, V, and Cr.

Imaging of Surface Segregation in Alloys

Lianfeng Zou¹ and Guangwen Zhou²

¹Pacific Northwest National Laboratory, Richland, Washington, United States, ²SUNY Binghamton University, Binghamton, New York, United States

Although phase diagrams delineating the thermodynamic conditions for phase selection in bulk alloys are well established, the composition and structure of an alloy surface can be significantly different from those of the bulk due to surface segregation of the alloying element. Often, such minor compositional modifications can lead to drastic changes in properties: at free surfaces these changes can affect corrosion resistance and catalytic function; at grain boundaries they influence fracture strength; at dislocations they alter plastic deformation behavior; and at heterophase interfaces they affect adhesion and integrity. Current understanding of surface segregation phenomena has largely relied on ultrahigh vacuum (UHV)-based surface science tools that give a mean value of surface composition averaged over a few atomic layers below the surface. Meanwhile, important surface structure information is usually missed from the composition measurements by surface spectroscopic tools.

Surface segregation usually extends deeper than the outermost layer and may be accompanied by both compositional and structural changes that extend several atomic layers below the surface. Dynamic depth-resolved probing of segregation has always been a major challenge. Particularly, monitoring segregation induced structural evolution is barely achieved because of experimental difficulties in spatially and temporally resolving both structure and composition in the surface and subsurface. Environmental transmission electron microscopy (E-TEM) is one of the few tools capable of monitoring surface structure and composition evolution by applying stimuli to drive segregation. The work presented therefore encompasses an atomic-scale study by exploiting the unique in situ capabilities E-TEM to dynamically monitoring the segregation-induced structural changes in both the surface and subsurface, at the atomic scale and in real time, in response to environmental stimuli.

Fig. 1(a-c) exemplifies time-sequence HRTEM images showing Au-segregation induced nucleation and growth of a half-unit-cell thick $L1_2$ $\text{Cu}_3\text{Au}(110)-(2\times 1)$ surface alloy by annealing a Cu–10at.% Au solid solution at 350°C and 1×10^{-3} Torr of H_2 gas flow. The (100) and (110) facets intersect at a corner area (Fig. 1a). The HRTEM image shows that both the (100) and (110) facets are initially of a non-reconstructed (1×1) structure with a flat morphology. A small high-index facet begins to form at the corner area via lateral decay of the (100) facet, accompanied by the segregation of Au atoms to the surface and subsurface regions of the high-index facet in the corner. Au atomic columns appearing in dark contrast are marked with white dashed rings and are numbered, as shown in Fig. 1(b). Au atoms continue to segregate in the corner area adjacent to the Cu_3Au nucleus, leading to the lateral growth of the $\text{Cu}_3\text{Au}(110)$ surface alloy (Fig. 1(c)). Fig. 1(d-f) presents another time sequence of in-situ HRTEM images showing the evolution of microfacets leading to the stable $\text{Cu}_3\text{Au}(110)-(2\times 1)$ surface structure. Fig. 1(d) corresponds to the beginning of the sequence, where the $\text{Cu}_3\text{Au}(110)-(2\times 1)$ segment borders with a high-index (410) facet (the blue arrow points to the location where they meet). The (410) facet does not present as a stable structure and undergoes changes induced by fast attachment and detachment of atoms at the step edges. The (100) terraces within the (410) facet are observed to decay via step-edge detachment of surface atoms. As a result, the (410) unit that borders with the $\text{Cu}_3\text{Au}(110)-(2\times 1)$ segment transits to a (420) configuration (Fig. 1(e)). The (420)/(410) stepped facet shows structural fluctuations as additional atoms diffuse in and out. The detachment of the four atomic columns (circled by yellow rings in Fig. 1(e)) at the step-edge area of the (420) facet, together with the decay of the (100) terrace (atomic columns circled by red rings in Fig. 1(e)) of the (410) facet, results in the lateral growth of the $\text{Cu}_3\text{Au}(110)-(2\times 1)$ segment by one-unit-cell length, with the concomitant formation of a new (420) facet to border with the front of the $\text{Cu}_3\text{Au}(110)-(2\times 1)$ segment. By following the same transformation path that involves structural fluctuations of the (420)/(410) stepped facets and the decay of the (100) terraces within the

stepped facets, the Cu_3Au surface alloy is seen to propagate toward the bottom-right corner direction (Fig. 1(f)). Our atomistic simulations demonstrate that the (2×1) reconstruction of the $\text{Cu}_3\text{Au}(110)$ surface alloy remains as a stable surface structure as a result of the favored Cu-Au diatom configuration [1]. The resulting surface segregated layer [1] is found to have a profound effect on surface properties including acting as an effective barrier to inhibit dislocation annihilation at free surfaces [2] and significantly slow down surface oxidation [3, 4].

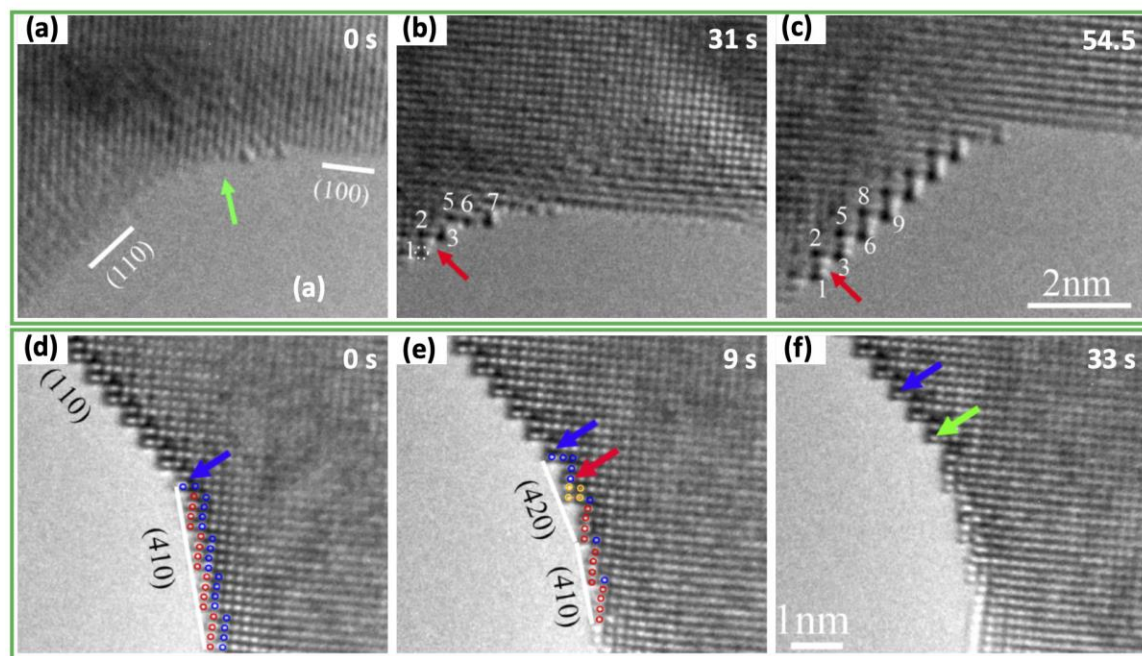


Figure 1. (a-c) Time-resolved HRTEM images showing the nucleation and growth of the half-unit-cell thick L12 ordered $\text{Cu}_3\text{Au}(110)-(2\times 1)$ surface alloy out of the Cu-10at.% Au solution at 350oC and 1×10^{-3} Torr of hydrogen gas flow. Au-rich atomic columns are marked by dashed circles. The red arrows point to the first nucleated Cu_3Au unit. (d-f) Time-sequence HRTEM images showing the structural transition pathway leading to the growth of the ordered $\text{Cu}_3\text{Au}(110)-(2\times 1)$ reconstruction at 350oC and 1×10^{-3} Torr of hydrogen gas flow. Red and blue rings denote the atoms that remain and diffuse away, respectively, in each next sequence. The blue arrows point to the same position in all the images, which is the end of the $(110)-(2\times 1)$ segment at the beginning of the sequence. The red and green arrows point to the new front of the (2×1) segment.

References

- [1] Zou, L., et. al., *J. Phys. Chem. Lett.* 8 (24), 6035 (2017)
- [2] Zou, L. et. al., *Nat. Mater.* 17, 56 (2018)
- [3] Zou, L. et. al., *Acta Mater.* 154, 220 (2018)
- [4] This work was supported by the National Science Foundation (Award No: DMR-1905422)